

A New Overloading Fatigue Model for Ergonomic Risk Assessment with Application to Human-Robot Collaboration

Marta Lorenzini^{1,2}, Wansoo Kim¹, Elena De Momi², and Arash Ajoudani¹

Abstract— Among the numerous risk factors associated to work-related musculoskeletal disorders (WMSD), repetitive and monotonous movements with light-weight tools are one of the most frequently cited. Such tasks may indeed result in the excessive accumulation of local muscle fatigue, causing severe injuries in human joints. Accordingly, this paper proposes a new whole-body fatigue model to evaluate the cumulative effect of the overloading torque induced on the joints over time by light payloads. The proposed model is then integrated into a human-robot collaboration (HRC) framework to set the timing of a body posture optimisation procedure guided by the robot assistance, by the time fatigue overcomes a threshold in any joint. Our overloading fatigue model is based on an estimation method we developed in a previous work, to monitor joint torque variations due to external forces in real-time. To account for individuals' different perception of fatigue, the fatigue ratio parameter in the model is computed experimentally for each subject. The proposed model is first studied on ten subjects by means of an electromyography analysis. Next, its performance is assessed in a painting task and finally evaluated within the HRC framework, which is proved to be able to reduce the risk of injuries caused by excessive fatigue accumulation.

I. INTRODUCTION

There is a growing awareness of the need to reduce work-related musculoskeletal disorders (WMSDs) in industrial countries, with the aim to decrease consequent substantial costs and impacts on the quality of life [1]. In this direction, several methods have been proposed to assess human exposure to risk factors associated to WMSDs [2], with repetitive and monotonous movements among the most frequently cited in both experimental science and epidemiologic investigations [3]. In fact, repetitive motions with light-weight objects may result in the accumulation of local muscle fatigue, which can cause severe injuries [4], [5], similarly to the manual handling of heavy loads in workspaces. Therefore, models to estimate cumulative fatigue due to repetitive workload and methods to mitigate its negative effects, are two major requirements towards the prevention of WMSDs.

To predict an individual's progression of fatigue over time, several models have been proposed in literature. The examples include modelling of Ca^{2+} cross-bridge mechanism [6], the force-pH relationship [7], and motor units voluntary activation [8]. Such physiological models are among the most precise tools to identify human fatigue levels, but maybe too complex for occupational ergonomics, which demands for practical (i.e., fewer subject-specific parameters) and computationally light approaches.

¹HRI² Lab, Department of Advanced Robotics, Istituto Italiano di Tecnologia, Genoa, Italy, Email: marta.lorenzini@iit.it, wan-soo.kim@iit.it

²Department of Electronics, Information and Bioengineering, Politecnico di Milano, Milano, Italy

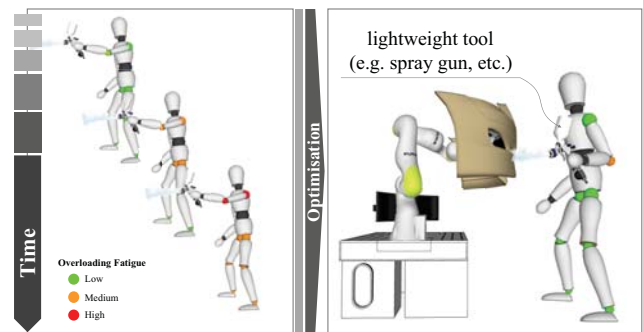


Fig. 1: In this work we propose a novel HRC framework to prevent excessive progression of fatigue while performing a repetitive manufacturing task with a light-weight tool.

On the other hand, it has been demonstrated that significant biochemical and physiological changes in fatigued muscles can be detected by analysing surface electromyography (sEMG) signals [9], [10]. A large portion of these works has focused on quantifying muscle fatigue in isometric contractions, with the extension to dynamic cases only during the last decade [11], [12]. Nevertheless, the use of sEMG presents several drawbacks. Firstly, a correct placement of the EMG sensors is not simple and a sEMG signal that originates in the muscle is inevitably affected by various noise signals or artifacts [13]. Secondly, the relative movement of the electrodes with respect to the measured muscle during the sEMG measurements in dynamic conditions makes their estimates questionable and may lead to incorrect conclusions [14]. Moreover, if a person dynamically interacts with the external environment, the frequency spectrum of the EMG signal, which is a well-known tool to analyse muscle fatigue, is strongly affected. Hence, the application of sEMG signals in estimating fatigue in dynamic Human-Robot Collaboration (HRC) tasks can be limited [15]. Finally, a direct estimation of muscular fatigue can be obtained from the measurement of the reduction of muscular strength or force output when exerting against an external load for a period of time. The reduction of the muscular strength, that is often associated to the maximum voluntary contraction (MVC), can be estimated by fitting a certain function, with exponential models among the most common [16]–[18]. The application of this concept in identifying a joint-level fatigue has been reported in [19]. Its extension to a larger number of joints (whole-body), however, can be challenging due to the use of several subject-specific parameters. In fact, most studies in this context extract the required data from anatomic tables, making the cross-subject accuracy of the method questionable.

Accordingly, the aim of this paper is to propose a whole-

body and subject-specific model to identify an individual's fatigue progression over time while performing repetitive tasks involving light payloads. The method is based on our previous work [20], in which we presented a real-time model to monitor human joint torque variations while holding heavy objects. A principled simplification approach was used here which neglects the gravity effect but reduces the number of subject parameters to be identified, avoiding the use of standard data and, above all, it addresses real-time compatibility. Such a model was integrated in a HRC control framework, by which a collaborative robot continuously adjusted the human counterpart's postures to perform a heavy manipulation task in an ergonomic way [21].

A direct application of our previous method would not be suitable in the mitigation of risks associated to repetitive light-weight tasks since the estimated overloading joint torques are low/moderate and the associated risk of joint injuries is not high. Consequently, the optimisation of the body configuration is not necessary and, on the contrary, could affect the efficiency of the workers in performing their tasks¹. On the other hand, even if the instantaneous overloading torques are not significant, the building up of their effect on the joints over a protracted period of time could become hazardous. Hence, the focus of this work is to develop a new fatigue model which takes into account such a cumulative impact of the overloading joint torque throughout time. The proposed overloading fatigue model is then used to set an appropriate timing for the body posture optimisation procedure, and to provide appropriate robotic assistance as soon as the estimated fatigue overcomes a predefined threshold (see Fig. 1). The presented fatigue model is first validated on ten subjects and then the robot optimisation framework is evaluated experimentally with one subject as a proof of concept, to illustrate its potential to improve worker ergonomics in performing their daily repetitive tasks, and to impact their productivity and welfare.

II. OVERLOADING JOINT FATIGUE

This section introduces our new overloading fatigue model. The proposed model estimates the progression of fatigue by taking into account two major factors: the variability of the overloading on the joints in presence of an external force, and an individual's subjective perception of fatigue. Taking advantage of an estimation method we developed in a previous work, our fatigue model reflects the variations of overloading torques on the joints due to an external payload (yet neglecting gravity effect) in any arbitrary body configuration. Hence, different values of external forces or payloads, or the changes of body configuration will result in different joint overloadings and a different rate of fatigue accumulation. In addition, since the perception of fatigue is expected to be subject-specific, an index called fatigue ratio K is considered in our model, which is computed

¹To our knowledge, there is little research carried out on the implementation of practical strategies to help preventing the accumulation of excessive fatigue, which are mostly based on work/rest schedules [11] or focused on specific applications [19].

experimentally. The less the subjects can support a load, the greater the fatigue ratio K and the quicker the accumulation of joint fatigue.

The overloading joint torques² can be obtained based on the human whole-body centre of pressure (CoP) and ground reaction forces (GRF) variations in the support plane (x - y) which are computed between two conditions, i.e., with and without the presence of external forces [20]. If the external load is not known, a force-plate or sensor insoles are required to compute the CoP values in the loading condition. Otherwise, an extended algorithm was developed by our team to calculate the effect of loading on CoP and GRF variations, without the need for external (force-pressure) sensory systems [22]. This approach is feasible when the external loads are known in advance. Since a painting task with a spray gun with a known mass and inertial properties is considered in this paper, the algorithm developed in [22] is used for the online estimation of the overloading torques.

A. Fatigue and Recovery model

The proposed overloading joint *fatigue model* is based on the joint torque capacity and the overloading effect on the given joints. Similarly to [19], the fatigue model can be represented by an RC circuit with zero initial charge state, which is mathematically modelled by a differential equation. The overloading joint fatigue of the i -th joint τ_i^F at a time instant t can be defined as:

$$\tau_i^F(t) = \tau_i^{\max} \left(1 - e^{-K_i \int_0^t \frac{\tau_i^\Delta(t)}{\tau_i^{\max}} dt} \right), \quad (1)$$

where τ_i^{\max} is the maximum joint overloading for the i -th joint, chosen from the biomechanical data, K_i is the fatigue ratio for the i -th joint (see subsection II-B for details), and $\tau_i^\Delta(t)$ is the overloading torque for the i -th joint at a time instant t , which is obtained by the generalised coordinates \mathbf{q} of a floating base human model: $\mathbf{q} = [\mathbf{x}_0^T \ \boldsymbol{\theta}_0^T \ \mathbf{q}_h^T]^T \in \mathbb{R}^{6+n}$. \mathbf{x}_0^T , $\boldsymbol{\theta}_0^T$ and $\mathbf{q}_h \in \mathbb{R}^n$ represent the position, the orientation of the base frame w.r.t the inertial frame and the angular position of n human joints, respectively.

Along with the overloading joint fatigue model, a *recovery model* should also be modelled to describe how the force generation capacity is recovered during rest periods. The recovery model can be defined as:

$$\tau_i^F(t) = \tau_i^{\max} - (\tau_i^{\max} - \tau_i^{F_0})e^{-R_i t}, \quad (2)$$

where $\tau_i^{F_0}$ is the initial value of the overloading fatigue and R_i is the recovery ratio for the i -th joint, which is set to $2.4K_i$ in accordance with other works on recovery models found in literature [8], [17].

In the new proposed overloading joint fatigue and recovery models, we assume that the relationship between the models is represented by the threshold $\tau_i^{\text{th}} = 0.33\tau_i^{\max}$. The model

²The details of the method can be found in [20], and will not be repeated here due to the page limits.

can then be defined as:

$$\tau_i^F(t) = \begin{cases} \text{Fatigue model} & \text{if } \tau_i^\Delta(t) > \tau_i^{\text{th}} \\ \text{Recovery model} & \text{otherwise} \end{cases}.$$

B. Fatigue ratio identification

Since fatigue is strictly related to the subject's physical capacity and feelings, the fatigue ratio K_i must be subject-specific and can be identified experimentally, for each i -th joint. To obtain this ratio, we consider the overloading fatigue model in static conditions, resulted from a constant overloading joint torque in a fixed body configuration. A time interval T_F is defined, similarly to the maximum endurance time (MET) presented in [23], by the period from the beginning of the trial to the time instant at which joint overloading fatigue reaches the current overloading torque $\bar{\tau}_i^\Delta$ at joint i . Hence:

$$\tau_i^F(t) = \tau_i^{\text{max}} \left(1 - e^{-K_i \|\bar{\tau}_i^\Delta\| T_F} \right) = \bar{\tau}_i^\Delta, \quad (3)$$

where $\|\bar{\tau}_i^\Delta\|$ is the normalised current overloading joint torque, defined as $\bar{\tau}_i^\Delta / \tau_i^{\text{max}}$. Consequently, the fatigue ratio K_i is obtained from the measured T_F in (3) as

$$K_i = - \frac{\ln(1 - \|\bar{\tau}_i^\Delta\|)}{\|\bar{\tau}_i^\Delta\| T_F}. \quad (4)$$

The fatigue ratio K_i is computed for each i -th joint since the strength exerted by each joint varies and thus the fatigue occurs in different timings.

III. VERIFICATION OF THE METHOD

This section first describes the procedure for the identification of the fatigue ratio, K_i . Next, the results of the overloading fatigue model are evaluated by means of a sEMG signal analysis in static conditions. The capability of the model to monitor the progression of fatigue in real-time is then presented for ten subjects performing a painting task with a light-weight tool. Finally, the proposed model is integrated into the HRC framework we presented in [21] to set the timing for the body configuration optimisation and thus to trigger the collaborative robot assistance by the time fatigue is accumulated excessively in some joint.

A. Model identification

Ten healthy volunteers, 7 males and 3 females, (age: 30.1 ± 3.8 years; mass: 65.5 ± 29.5 kg; height: 176.2 ± 5.2 cm) were recruited in the experimental session. A written informative consent was obtained after explaining the experimental procedure. To identify K_i by means of (4), the subjects had to keep a defined position until they were able to support a load without changing even minimally the body configuration. In this way, we could assume that the overloading joint torque $\bar{\tau}_i^\Delta$, which is function of the body configuration and external load, was constant throughout the experiment. The time interval, defined as T_F , since the subjects started holding the load till when they were no longer able to support it, i.e. when they reached a high level of fatigue, was measured. We first compute the fatigue ratio

K_s for the shoulder joint, given the value of the correspondent overloading joint torque $\bar{\tau}_s^\Delta$ in the selected body configuration. To this aim, the subjects were asked to stand and hold a 1.5 kg weight (corresponding to the weight of the painting tool) with the dominant hand, having the arm raised at a 90-degrees angle with the torso and the elbow slightly bended, the other arm by their side. The fatigue ratio for the other joints K_i could then be obtained proportionally, on the basis of the ratio between the maximum overloading joint torque for the shoulder τ_s^{max} and the maximum overloading joint torque for the i -th joint τ_i^{max} .

The evaluation of the proposed overloading fatigue model was conducted by comparing its outcomes to physiological fatigue expressed as the variations of the mean power frequency (MPF) of some significant sEMG signals. In fact, muscle fatigue during submaximal, i.e. isometric contractions, has been shown to be accompanied by decreases in the MPF [24]. Six sEMG sensors were placed on the arm of each subject, specifically on the following muscles: the anterior deltoid (AD), the posterior deltoid (PD), the biceps (BC), the triceps (TC), the brachioradialis (BR) and the extensor carpi ulnaris (EC). To monitor the current overloading torque, the subjects were asked to wear a MVN Biomech suit (Xsens Tech) provided with seventeen inter-connected inertial measurement unit (IMU) sensors to measure the whole-body motion. Then, they were asked to assume the same body configuration described above (for the fatigue ratio identification experiment) and to perform three trials: to hold the 1.5 kg weight without changing the defined position for three different time interval, respectively 90, 60 and 30 seconds, with the necessary rest time in between. During these trials, the sEMG signals were measured and the overloading joint fatigue was estimated by means of our algorithm. Prior to the analysis, the sEMG signals were filtered (pass band: 1-500 Hz) to remove movement artifacts. Linear regression was then used to extract from the sEMG data the linear model for the MPF, in accordance with studies for EMG-based fatigue analysis in literature [25], [26]. Both the MPF and the overloading fatigue time series were compressed to correspond to the same number of samples for the sake of comparison and the overloading fatigue values were normalised between 0 and 1. It is important to point out that MPF gives a fatigue estimation at the muscle level while our overloading fatigue model is expressed at the joint level. Since the joint motion is the result of several muscles contributions, the effect of several MPF components in the muscles acting on a specific joint must be considered to account for the joint-level fatigue. For this reason, a direct comparison between the two variables is not valid but the assessment of their similarities in the percentage of decrement/increment and in the trend could be a good way to compare the two.

Fig. 2 shows the results for one selected subject. The first line of graphs is related to the variables representative for the shoulder, i.e. the MPF decrement in the AD and PD muscles and the estimated normalised overloading fatigue $\|\tau_s^F\|$ in the shoulder joint. The second line of graphs, instead, is

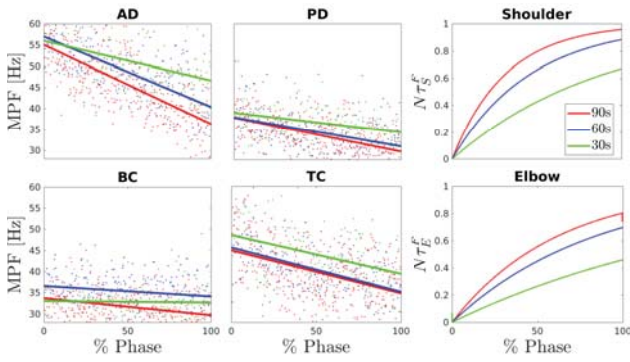


Fig. 2: Trend of the the MPF of the sEMG signals measured in the anterior deltoid (AD), posterior deltoid (PD), biceps (BC) and triceps (TC) muscles and trend of the overloading joint fatigue estimated in the shoulder and in the elbow throughout 3 different trial lasting 90, 60 and 30 seconds respectively, for one subject.

related to the variables representative for the elbow, i.e. the MPF decrement in the BC and in the TC muscles and the estimated normalised overloading fatigue $\|\tau_S^E\|$ in the elbow joint. The MPF trend in the BR and in the EC muscles were in the end considered not significant for our analysis. As we could expect, a longer trial corresponds to a greater decrement of the sEMG signals MPF in all the considered muscles and the overloading fatigue model is able to reproduce the same trend but, clearly, in the opposite way, since the progression of fatigue is described through an increasing function in our method. Due to space restrictions, we cannot show the results for all the ten subjects thus we computed the mean and the standard deviation of the decrement ratio for both the MPF and the overloading fatigue between all the subjects in the three experimental conditions. We performed a t-test and it resulted that all the analysed data come from a normal distribution at the 1% significance level, hence, we can consider the mean and the standard deviation as good indicators for our analysis. The results for the shoulder joint are presented in Table I while the results for the elbow joint are presented in Table II. The overloading fatigue model presents in all the subjects a increment trend comparable to the decrement trend of the sEMG signals MPF

TABLE I: Mean and standard deviation computed between ten subjects of the MPF of the sEMG signals measured in the anterior deltoid (AD) and posterior deltoid (PD) muscles and of the overloading joint fatigue estimated in the shoulder in 3 trials lasting 90, 60 and 30 seconds, respectively.

Period	EMG % dec.		Fatigue % inc.
	AD	PD	Sho
90s	24.92±10.08	20.06±8.74	94.42 ± 10.38
60s	16.45±12.71	15.73±9.78	87.48±14.24
30s	6.90±9.65	4.02±9.02	65.32±14.56

TABLE II: Mean and standard deviation computed between ten subjects of the MPF of the sEMG signals measured in the biceps (BC) and triceps (TC) muscles and of the overloading joint fatigue estimated in the elbow for 3 trials lasting 90, 60 and 30 seconds, respectively.

Period	EMG % dec.		Fatigue % inc.
	BC	TC	Elb
90s	8.27±7.50	19.48±5.20	57.03 ± 8.13
60s	4.47±9.80	14.81±7.58	46.43±8.45
30s	-0.34±6.91	6.21±8.54	31.97±8.77

in the three experimental conditions. We tested our overloading fatigue model performance by executing isometric, i.e. constant length (static) muscle contractions because sEMG measurements can be considered far more reliable in such conditions and can be used for evaluations. Nevertheless, as previously said, in dynamic conditions sEMG estimations are questionable while our model has the potential to be employed even in the dynamic case, i.e. when the subject moves to perform a task or applies different forces at hand.

B. Overloading fatigue real-time monitoring

The objective of the overloading fatigue model is to estimate the fatigue risk associated to repetitive light-weight task in real-time and then to promote a mitigation of such a risk in real-life environment. Hence, we have selected a real-life scenario in the manufacturing industry: manual spray painting, and proved the capability of the overloading fatigue model to monitor the progression of fatigue in real-time for different body configurations as well as the joints overloading. Such a task which consists in a high rate of repetitive work with a short cycle time and light-weight tool, has resulted in a high incidence of WMSDs [27], hence it could be a good candidate for the application of the proposed HRC framework to prevent the accumulation of fatigue.

Accordingly, the subjects, wearing the MVN Biomech suit, were asked to hold a 1.5 kg spray gun with their dominant hand and stand in front of a car bumper (the object which needed to be painted) placed approximately at the height of their torso. Next, following a set of sound signals which dictated a specific timing, they were asked to simulate the painting action with a spray gun in eight predefined points on the car bumper (i.e. P1, P2, ..., P8), in accordance with a specific order (see Fig. 3a). After the starting signal, the subjects had to process each point for approximately 15 second and, as soon as they heard another sound signal, they were asked to change body configuration to pass to the subsequent point as quickly as possible. The overloading fatigue in the crucial human joints was estimated throughout the experiment for all the subjects and its values was normalised between 0 and 1. We focused on the human body motion on the sagittal plane since it is the mainly involved in the activity we analysed. In addition, given that the movements of the leg were almost symmetric, we have assumed the overloading torque on the joints of the legs to be equal in the right and in the left one.

In Fig. 3b we show the normalised overloading torque $\|\tau^A\|$ (left side) and the normalised overloading fatigue $\|\tau^F\|$ (right side) in the shoulder (S) and in the elbow (E) - the joints more at risk for this specific task - for one subject. These graphs show how the trend of the overloading fatigue varied depending on the value of the overloading torque: if $\|\tau^A\|$ was over the threshold, $\|\tau^F\|$ increased while it decreased under the threshold since the recovery mode was initiated. It is worth noticing here the capability of the overloading fatigue model to account for the cumulative effect of the overloading torque throughout time. Considering the elbow joint for example, the overloading torque value

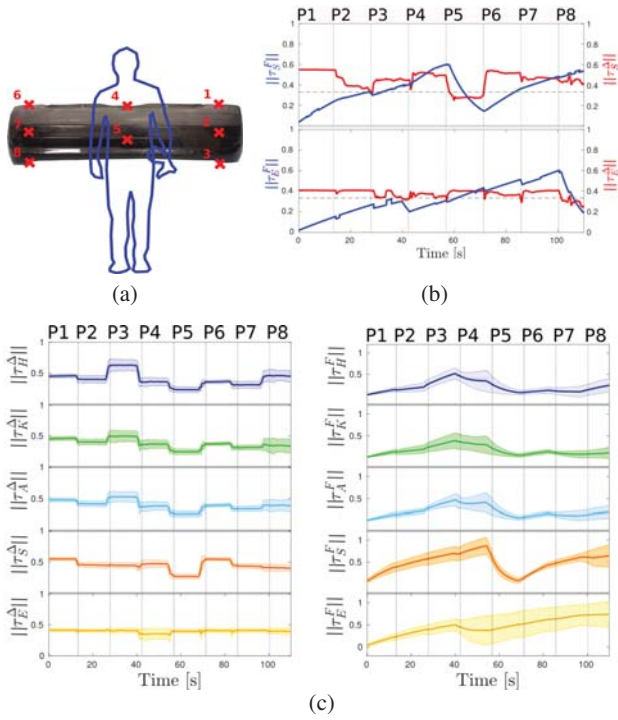


Fig. 3: Overloading fatigue monitoring: (a) experimental setup; (b) overloading joint torque (red line) and overloading joint fatigue (blue line) estimated in the shoulder (S) and in the elbow (E) for one subjects; (c) mean and standard deviation of the overloading joint torque (left side) and of the overloading joint fatigue (right side) computed between ten subjects in the main body joints: hip (H), knee (K), ankle (A), shoulder (S) and elbow (E).

remained moderate and almost constant over the entire duration of the task thus it did not represent a potential source of risk. On the other hand, the overloading fatigue took into consideration its cumulative contribution and, after some time, its value was increased significantly. Fig. 3c presents the results of the joint overloading torque (left side) and of the fatigue (right side) between the ten subjects. It is evident that the trend of the overloading torque was very similar between the subjects since the timing of the task was fixed and the body configurations chosen by the subjects were very similar. The overloading fatigue, instead, is more variable since it depends even on the subject-specific fatigue ratio K .

C. Overloading fatigue mitigation through HRC

The overloading fatigue model was integrated in a HRC framework to trigger the collaborative robot assistance. By the time overloading fatigue exceeded a predefined threshold in a joint, the robot reacted and guided the subject towards a more ergonomic body configuration, to prevent further accumulation of fatigue. To estimate such optimal body configurations and consequently to set the robot trajectory, we employed an optimisation procedure that we developed in a previous work. Since fatigue accumulated due to the overloading effects, the cost of the optimisation had to consider the overloading joint torques with respect to body configuration. Hence, we defined a cost function and minimised it, implementing the optimisation problem as:

$$\min_{\mathbf{q}_h} \|\Delta\boldsymbol{\tau}^T \mathbb{W} \Delta\boldsymbol{\tau}\|, \quad (5)$$

where $\Delta\boldsymbol{\tau}$ is the overloading joint torque vector $\Delta\boldsymbol{\tau} = [\tau_1^\Delta \ \dots \ \tau_n^\Delta] \in \mathbb{R}^n$ and \mathbb{W} is a symmetric positive definite weight matrix. Several constraints, such as joint limits of the human, postural stability of the human, the position of the object, etc. (a detailed explanation can be found in [21]), were considered in the numerical optimisation process. As a result, an optimal body configuration was computed and robot trajectories were adjusted accordingly, to facilitate the subject to achieve such ergonomic configurations.

One female subject (age: 27 years; mass: 57 kg; height: 171 cm) was recruited for the HRC experiment. She was asked to wear the MVN Biomech suit, to hold a 1.5 kg spray gun with her dominant hand and to paint a predefined area on a car bumper. A KUKA Lightweight robot (LWR), provided with an impedance controller to ensure safety in HRC and equipped with a Pisa/IIT Softhand, was holding the car bumper that needed to be processed. In Fig. 4 the experimental setup is shown. Considering the painting area which is highlighted in the picture (yellow area on the car bumper), the subject was anticipated to adopt a wide range of body postures to accomplish the task. For this reason, we expected different joints to accumulate fatigue in different phases of the task. Accordingly, the optimisation procedure had to occur multiple times throughout the task, and to focus selectively on the fatigued joint. As a support tool to the optimisation procedure, the subject was provided with a visual feedback we developed in a previous work [28], showing the current body configuration and the current level of the overloading fatigue on the main joints.

Fig.5a illustrates the four key moment of the experiment (i.e. stage 1, 2, 3, and 4). Some color-coded indicators are placed on the main joints of the subject to show the level of the overloading fatigue at that instant: high (red), medium (orange) and low (green) level. The trends of the normalised overloading fatigue in the main joints are presented in Fig. 5b. Initially, the subject began to process a point on the top of the car bumper by assuming a body configuration which made the shoulder joint accumulate excessive fatigue, as shown in the fourth line the graph in Fig. 5b. As soon as overloading fatigue overcame a threshold (stage 1), which is set to $1/2$ of the τ_i^{max} , the optimisation procedure was triggered

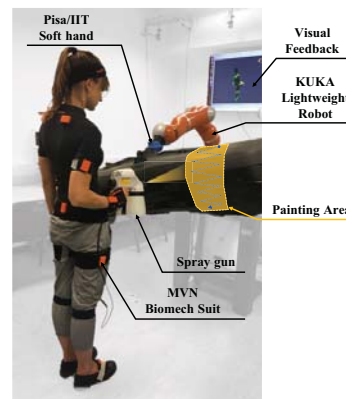


Fig. 4: Overloading fatigue mitigation through HRC: Experimental setup

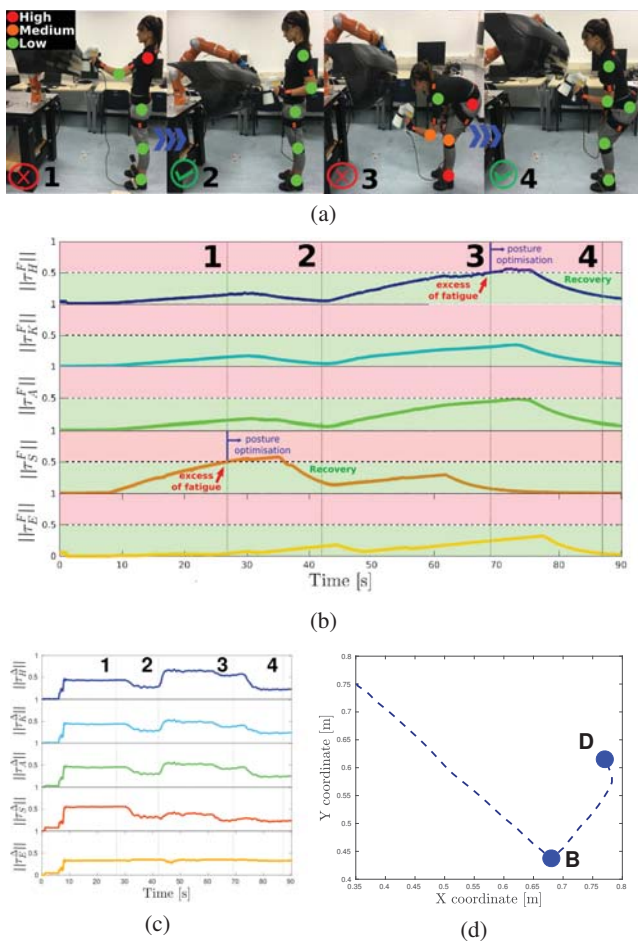


Fig. 5: Overloading fatigue mitigation through HRC: (a) Key moments of the HRC experiment. (b) overloading fatigue and (c) overloading torque in the hip(H), knee(K), ankle(A), shoulder(S) and elbow(E) joints for one subject performing the HRC experiment. (d) collaborative robot trajectory: the robot assistance promoted the recovery phase after fatigue in B and D.

and the subject was guided by the collaborative robot toward a more ergonomic body configuration, which led to a lower overloading torque in the shoulder and promoted the recovery phase (stage 2). In this case the optimisation procedure was more focused on the upper body and resulted in a decrement of the overloading fatigue in the shoulder. In Fig. 5d the trajectory of the collaborative robot end-effector is shown: to made the subject reach the optimal body configuration the car bumper is brought at a lower height at stage 2. Subsequently, the subject started processing a point on the bottom of the car bumper by assuming a body configuration which, this time, made the lower body accumulate fatigue (stage 3), mainly in the hip joint, as shown in the first line of the graph in Fig. 5b. Similarly, as soon as the overloading fatigue overcame the threshold, the optimisation procedure was triggered and the subject was guided by the collaborative robot toward a body configuration which led to a minor overloading torque in the lower body joints and initiate again the recovery mode (stage 4). In this case the optimisation procedure was more concentrated in the lower body and made the overloading fatigue decrease in the hips, knees and ankles. To this aim, the collaborative robot brought the car bumper at a higher

height at stage 4 (see Fig. 5d).

Fig. 5c presents the trends of the normalised overloading torque in the main joints. It is worth noticing that the values of the overloading torque remained moderate (around the 50% of their maximum value) in all the joints throughout the entire duration of the experiment. In our previous work [21], the optimisation procedure was performed when the overloading torque reached a value close to the maximum one, since heavy tools which generated high overloadings were considered. In this work, we consider a light-weight tool and the overloading torques it induces on the joints are not so high. Hence, the optimisation procedure would not be initiated in our previous framework. In fact, as previously mentioned, the risk of joint injuries while supporting light payload is not related to the instantaneous loading they induce, but rather on their prolonged and repeated use over time. This is the reason why we developed an overloading fatigue model which accounts for the cumulative effect of the overloading torque throughout time and thus represents a good criterion to set the timing of the optimisation procedure when performing task with light-weight tool.

IV. CONCLUSIONS AND FUTURE WORK

In this paper we developed a whole-body fatigue model to account for the cumulative effect of the overloading torque exerted on the joints over time by light payloads. The proposed model is able to monitor in real-time the progression of fatigue, whose trend varies on the basis of the external load and body configuration. In comparison to the EMG-based fatigue models that lack robustness due to the external noise, our approach can effectively monitor the progression of fatigue during dynamic interactions with the external world. If the mass and the inertial properties of the load are known, the sensory system required to account for the whole-body fatigue is reduced to the tracking of human motion and this substantially increases the applicability of the proposed method in industrial settings. The insignificant dependency of our model on the biomechanical tables and its ability to provide subject-specific fatigue progression, reflecting an individual's perception of fatigue, are additional strong points of the proposed method.

To implement a practical strategy for preventing joint injuries caused by repetitive and prolonged tasks with light-weight tools, we integrated the overloading fatigue model in a HRC framework. By the time fatigue exceeded a threshold in any joint, a body posture optimisation was triggered, guided by the collaborative robot assistance, and the accumulation of further fatigue was avoided.

Future works will focus on an adaptive HRC framework which can handle tasks performed with both light-weight and heavy tools, taking into account the corresponding risk factor, i.e. the fatigue accumulation or the excessive mechanical overloading on the body joints, respectively. Such a framework will be evaluated through quantitative physiological measurements (i.e., oxygen consumption for fatigue assessment) and questionnaires completed by the subjects to improve its performance and feasibility.

REFERENCES

- [1] L. Punnett and D. H. Wegman, "Work-related musculoskeletal disorders: the epidemiologic evidence and the debate," *Journal of electromyography and kinesiology*, vol. 14, no. 1, pp. 13–23, 2004.
- [2] G. David, "Ergonomic methods for assessing exposure to risk factors for work-related musculoskeletal disorders," *Occupational medicine*, vol. 55, no. 3, pp. 190–199, 2005.
- [3] B. P. Bernard and V. Putz-Anderson, "Musculoskeletal disorders and workplace factors; a critical review of epidemiologic evidence for work-related musculoskeletal disorders of the neck, upper extremity, and low back," 1997.
- [4] J. Potvin and R. Norman, "Quantification of erector spinae muscle fatigue during prolonged, dynamic lifting tasks," *European journal of applied physiology and occupational physiology*, vol. 67, no. 6, pp. 554–562, 1993.
- [5] H.-J. Shin and J.-Y. Kim, "Measurement of trunk muscle fatigue during dynamic lifting and lowering as recovery time changes," *International journal of industrial ergonomics*, vol. 37, no. 6, pp. 545–551, 2007.
- [6] J. Ding, A. S. Wexler, and S. A. Binder-Macleod, "A predictive fatigue model. i. predicting the effect of stimulation frequency and pattern on fatigue," *IEEE Transactions on Neural Systems and Rehabilitation Engineering*, vol. 10, no. 1, pp. 48–58, 2002.
- [7] Y. Giat, J. Mizrahi, and M. Levy, "A musculotendon model of the fatigue profiles of paralyzed quadriceps muscle under fes," *IEEE transactions on biomedical engineering*, vol. 40, no. 7, pp. 664–674, 1993.
- [8] J. Z. Liu, R. W. Brown, and G. H. Yue, "A dynamical model of muscle activation, fatigue, and recovery," *Biophysical journal*, vol. 82, no. 5, pp. 2344–2359, 2002.
- [9] C. L. De, "Myoelectrical manifestations of localized muscular fatigue in humans," *Critical reviews in biomedical engineering*, vol. 11, no. 4, pp. 251–279, 1984.
- [10] M. Cifrek, V. Medved, S. Tonković, and S. Ostojčić, "Surface emg based muscle fatigue evaluation in biomechanics," *Clinical Biomechanics*, vol. 24, no. 4, pp. 327–340, 2009.
- [11] E. Spyropoulos, E. Chroni, and G. Athanassiou, "Muscle fatigue estimation in repetitive lifting task using surface electromyography-based analysis," *Journal of Ergonomics*, vol. 5, 2015.
- [12] L. Peternel, N. Tsagarakis, D. Caldwell, and A. Ajoudani, "Robot adaptation to human physical fatigue in human-robot co-manipulation," *Autonomous Robots*, pp. 1–11, 2018.
- [13] C. J. De Luca, L. D. Gilmore, M. Kuznetsov, and S. H. Roy, "Filtering the surface emg signal: Movement artifact and baseline noise contamination," *Journal of biomechanics*, vol. 43, no. 8, pp. 1573–1579, 2010.
- [14] D. Farina and R. Merletti, "A novel approach for precise simulation of the emg signal detected by surface electrodes," *IEEE Transactions on Biomedical Engineering*, vol. 48, no. 6, pp. 637–646, 2001.
- [15] A. Ajoudani, A. M. Zanchettin, S. Ivaldi, A. Albu-Schäffer, K. Kosuge, and O. Khatib, "Progress and prospects of the human-robot collaboration," *Autonomous Robots*, pp. 1–19, 2018.
- [16] H. Iridiastadi and M. Nussbaum, "Muscle fatigue and endurance during repetitive intermittent static efforts: development of prediction models," *Ergonomics*, vol. 49, no. 4, pp. 344–360, 2006.
- [17] D. D. Wood, D. L. Fisher, and R. O. Andres, "Minimizing fatigue during repetitive jobs: optimal work-rest schedules," *Human factors*, vol. 39, no. 1, pp. 83–101, 1997.
- [18] L. Ma, D. Chablat, F. Bennis, and W. Zhang, "Dynamic muscle fatigue evaluation in virtual working environment," *International Journal of Industrial Ergonomics*, vol. 39, no. 1, pp. 211–220, 2009.
- [19] L. Ma, D. Chablat, F. Bennis, W. Zhang, and F. Guillaume, "A new muscle fatigue and recovery model and its ergonomics application in human simulation," *Virtual and Physical Prototyping*, vol. 5, no. 3, pp. 123–137, 2010.
- [20] W. Kim, J. Lee, N. Tsagarakis, and A. Ajoudani, "A real-time and reduced-complexity approach to the detection and monitoring of static joint overloading in humans," in *Rehabilitation Robotics (ICORR), 2017 International Conference on*. IEEE, 2017, pp. 828–834.
- [21] W. Kim, J. Lee, L. Peternel, N. Tsagarakis, and A. Ajoudani, "Anticipatory robot assistance for the prevention of human static joint overloading in human-robot collaboration," *IEEE Robotics and Automation Letters*, vol. 3, no. 1, pp. 68–75, 2018.
- [22] L. Peternel, W. Kim, J. Babič, and A. Ajoudani, "Towards ergonomic control of human-robot co-manipulation and handover," in *Humanoid Robotics (Humanoids), 2017 IEEE-RAS 17th International Conference on*. IEEE, 2017, pp. 55–60.
- [23] D. Imbeau, B. Farbos *et al.*, "Percentile values for determining maximum endurance times for static muscular work," *International Journal of Industrial Ergonomics*, vol. 36, no. 2, pp. 99–108, 2006.
- [24] V. Balasubramanian and S. Jayaraman, "Surface emg based muscle activity analysis for aerobic cyclist," *Journal of bodywork and movement therapies*, vol. 13, no. 1, pp. 34–42, 2009.
- [25] M. A. Nussbaum, "Static and dynamic myoelectric measures of shoulder muscle fatigue during intermittent dynamic exertions of low to moderate intensity," *European journal of applied physiology*, vol. 85, no. 3-4, pp. 299–309, 2001.
- [26] S. Thongpanja, A. Phinyomark, P. Phukpattaranont, and C. Limsakul, "Mean and median frequency of emg signal to determine muscle force based on time-dependent power spectrum," *Elektronika ir Elektrotechnika*, vol. 19, no. 3, pp. 51–56, 2013.
- [27] G. Björing and G. M. Hägg, "Musculoskeletal exposure of manual spray painting in the woodworking industry—an ergonomic study on painters," *International Journal of Industrial Ergonomics*, vol. 26, no. 6, pp. 603–614, 2000.
- [28] M. Lorenzini, W. Kim, E. De Momi, and A. Ajoudani, "A synergistic approach to the real-time estimation of the feet ground reaction forces and centers of pressure in humans with application to human-robot collaboration," *IEEE Robotics and Automation Letters*, vol. 3, no. 4, pp. 3654–3661, 2018.